Desalination and Water Treatment
www.deswater.com

doi: 10.1080/19443994.2013.873741

53 (2015) 3531–3542
March

Taylor & Francis
Taylor & Francis Group

Removal of aluminum from synthetic solutions and well water by chitin: batch and continuous experiments

Raphael Ricardo Zepon Tarpani[a], Flávio Rubens Lapolli[a], Maria Ángeles Lobo-Recio[a,b,*]

[a]*Water Reuse Laboratory, Department of Sanitary and Environmental Engineering, Technological Center, Universidade Federal de Santa Catarina, Campus Trindade, P.O. Box 476, Florianópolis, Santa Catarina 88040-970, Brazil*
[b]*Universidade Federal de Santa Catarina (UFSC), Campus Universitário de Araranguá, Unidade Jardim das Avenidas, Rodovia Governador Jorge Lacerda 3201, Araranguá, Santa Catarina 88900-000, Brazil*
Tel. +55 48 3721 7744/+55 48 3721 2198; Fax: +55 48 3234 6459; email: maria.lobo@ufsc.br

Received 11 June 2013; Accepted 2 December 2013

ABSTRACT

The intake of aluminum by humans is a matter of interest because it has shown potential association with health disorders, especially neurological complications, after long periods of chronic exposure. In this work, the removal of monomeric aluminum (Al^{3+}) from synthetic solutions and drinking well water using chitin as a sorbent agent was evaluated. Removal experiments in batch and in continuous regimes were carried out, along with isothermal and kinetic studies, which were performed to determine the adsorption mechanism and removal rates. Batch experiments demonstrated that 0.80 g chitin L^{-1} completely removed the Al^{3+} from synthetic solutions (concentrations upto 2.75 mg Al^{3+} L^{-1}) and from well water (upto 0.83 mg Al^{3+} L^{-1}). Isothermal studies in synthetic solutions demonstrated that the Al^{3+} removal via chitin was best fit by the Tóth isothermal model (maximum adsorption capacity of 20.14 mg Al^{3+} g^{-1} chitin), which is consistent with a chemisorption mechanism with weaker interactions than those proposed in the Langmuir model. The removal fitted pseudo-second-order kinetics, which is consistent with a chemisorption mechanism, showing a high initial adsorption rate. Descending flux column (flow 19.80 mL min^{-1}) experiments with well water resulted in a removal capacity of 9.53 mg Al^{3+} g^{-1}. Scanning electron microscopy/energy dispersive X-ray spectroscopy analysis revealed adsorption sites for aluminum along the chitin surface. Infrared spectroscopy did not show covalent bonds between the chitin and the aluminum in the samples, which is consistent with the isothermal studies.

Keywords: Drinking water; Aluminum removal; Chitin; Chemisorption

1. Introduction

Aluminum is present at different concentrations and in various species in water supply systems, and human contact with and ingestion of this element has increased significantly due to increasing industrialization, as aluminum is used in a wide variety of applications [1,2]. Studies have shown that the absorption of aluminum by the human body is often higher than that reported in early studies [3].

It is now recognized that aluminum can cause kidney and bone complications, lung disability and is

*Corresponding author.

associated with dementia-inducing diseases, such as Parkinson's and Alzheimer's diseases [4,5]. Difficulties in measuring low concentrations and identifying the mechanisms by which it reaches human tissues are obstacles to predicting or defining safe concentrations for human ingestion of this substance. The water supply has been demonstrated to contain the most hazardous species of aluminum, such as Al^{3+}, $Al(OH)_2^+$, and $AlOH^{2+}$ [3,6]. For drinking water, most countries have established a maximum permissible concentration value, determined by the World Health Organization (WHO), of 0.20 mg L^{-1} of total aluminum [7]. In view of this regulation, many studies have aimed to remove aluminum from water utilizing several different materials and techniques [8–12].

Based on literature, this study evaluated and analyzed Al^{3+} removal by the biopolymer chitin at concentrations commonly found in drinking water. Chitin is synthesized by a large number of living organisms and is the second most abundant biopolymer available in nature, after cellulose. Chitin is obtained through stringent purification procedures, which remove undesirable substances and may also cause modifications in its primary structure [13]. Chitin has N- and O-donor functional groups, enabling it to bond with highly polarized ions, such as Al^{3+} [14]. However, a derivative of chitin, chitosan, has become a more prominent biopolymer in recent studies regarding the removal of metal ions, even though it is easier and cheaper to produce chitin.

In our recent paper [15], the capacity to remove Al^{3+} from synthetic solutions of the biopolymers carboxymethylcellulose, chitin, and chitosan in batch regime was evaluated. It was concluded that chitin and chitosan showed similar high removal capacities, while carboxymethylcellulose was excluded as a potential removal agent of Al^{3+} at drinking water concentrations (assumed to be 0.05–3.00 mg Al^{3+} L^{-1}).

In the present work, focus was placed on further experiments with chitin, adding continuous regime experiments. Therefore, chitin was identified as a suitable material to remove aluminum from solutions through simple treatment process. Isothermal experiments (considering the Langmuir, Freundlich, Sips and Tóth models) were performed in synthetic solutions, and kinetic experiments (considering pseudo first-order, pseudo second-order and intra-particle diffusion models) were carried out in synthetic solutions and in well water. Continuous regime experiments were carried out to determine operational conditions for future implantation of this process at pilot or larger scales. Spectroscopic analysis allowed better evaluation of the interactions between aluminum and the biopolymer.

2. Materials and methods

2.1. Materials

Chitin was extracted from shrimp shells through purification procedures with hydrochloric acid (1.0 N HCl), sodium hydroxide (3% NaOH) and sodium hypochlorite (0.315% NaClO) at room temperature, then dried at 353 K for 4 h [13]. Next, the chitin was pulverized and sieved through 0.10 mm pores.

Experiments in synthetic solutions were carried out at predefined Al^{3+} concentrations that were prepared by adding alum ($Al_2(SO_4)_3$-(14–18)H_2O) to deionized water, with further dilution to reach the desired concentrations. The well water was kindly provided by a south Brazilian water company SAMAE (Araranguá, Santa Catarina, Brazil), with an Al^{3+} concentration of 0.83 mg L^{-1}. The drinking water treatment plant (DWTP) samples originated from a plant located in Jurerê International (Florianópolis, Santa Catarina, Brazil), which has conventional treatment procedures (coagulation, flocculation, sedimentation and filtration) utilizing alum as a coagulant, were collected from the step prior to filtration, showing an average concentration of 0.14 mg Al^{3+} L^{-1}.

All batch experiments were performed in a thermostatic bath, maintaining both the temperature and agitation constant at 298 K and 180 rpm, respectively, during the experimental period. To avoid the contamination of glassware with aluminum, high-density polypropylene Erlenmeyer flasks were used in the batch experiments. The descending flux column assays were carried out in glass columns of 80.0 cm height and 1.50 cm internal diameter, fed with well water by gravity. Due to the presence of aluminum in the laboratory environment, all glassware was rinsed with hydrochloric acid solution (HCl 1:1) and subsequently washed with distilled water, then left to dry at room temperature. All experiments were conducted in duplicate, and the pH was monitored but not controlled during experiments.

2.2 Methods

2.2.1. Analytical methods

A DR/2010 spectrophotometer (Hach CompanyLoveland, Colorado, United States) was used to measure the Al^{3+}, Fe_t, Mn_t, SiO_2, and SO_4^{2-} concentrations with Hach® colorimetric spectrophotometer kits. The colorimetric methods used were: Aluminon (detec-

tion range 0–0.80 mg L^{-1}, sensitivity 0.001 mg L^{-1}), PAN (detection range 0–1.300 mg L^{-1}, sensitivity 0.001 mg L^{-1}), PAN (detection range 0–0.700 mg L^{-1}, sensitivity 0.001 mg L^{-1}), Heteropoly Blue (detection range 0–1.60 mg L^{-1}, sensitivity 0.01 mg L^{-1}) and SulfaVer4 (detection range 0–70 mg L^{-1}, sensitivity 1.00 mg L^{-1}).

2.2.2. Batch isothermal and synthetic solution Al^{3+} removal experiments

Isothermal and Al^{3+} removal experiments were prepared by diluting a stock Al^{3+} solution in deionized water to produce samples containing different concentrations (ranging from 0.05 up to 3.00 mg Al^{3+} L^{-1}), as well as a blank sample. Then, 200 mL of each solution was poured in a 250 mL polypropylene Erlenmeyer flask with a pre-established amount of chitin (0.15 or 0.80 g L^{-1}) and then agitated in a thermostatic bath for 24 h to ensure that equilibrium was reached. After 24 h, the Erlenmeyer flasks were withdrawn, the contents were filtered in through a cellulose acetate filter (porosity 45 μm) and the corresponding concentrations of Al^{3+} were accurately measured.

In the previous paper [15], the Freundlich, Langmuir, and Sips isothermal models were considered to describe the experimental data and predict the adsorption mechanism, and the Sips model provided the best agreement. However, the difference between the R^2 values and the errors of the models were very narrow, and, consequently, this study includes one more model to describe the results, the Tóth model.

2.2.3. Batch kinetics and Al^{3+} removal experiments in synthetic solutions and well water

Kinetic and Al^{3+} removal experiments were conducted with synthetic solutions and well water samples. The desired chitin amount (0.15, 0.80 or 2.00 g L^{-1}) was added to10 Erlenmeyer flasks containing 200 mL of the chosen sample, and was stirred at 200 rpm and 25˚C for different amounts of time (from 5 to 1,440 min). At predetermined intervals, one Erlenmeyer flask was removed from the thermostatic bath, the content was filtered through a cellulose acetate filter (porosity 45 μm) and the filtrate was measured in terms of Al^{3+} concentration. The initial and final (after 24 h–end of the experiment) concentrations of Fe_t, Mn_t, SiO_2, and SO_4^{2-} were also measured in the well water.

2.2.4. Continuous regime studies

Adsorptive column studies were performed only with well water. The desired amount of biopolymer for each experiment was previously put in contact with deionized water, and then left to stand for a 24 h period in the column before the experiment began. Prior to the beginning of the experiment, the distilled water was withdrawn while the well water flux began. The feeding system was carried by gravity, with a well water reservoir connected to the column and the downward flow was controlled by the well water column above the chitin layer. At predetermined time intervals, 50 mL samples were measured for Al^{3+} content. The experiments ended when no significant variation between the input and output Al^{3+} contents of the column was detected. The initial and final (end of the experiment) concentrations of Fe_t, Mn_t, SiO_2, and SO_4^{2-} were also measured.

2.2.5. Instrumental analyses

The raw sieved chitin and Al^{3+}-saturated chitin were characterized by instrumental analysis method. To saturate the chitin with Al^{3+} from synthetic solution, the biopolymer was put in contact with a synthetic solution containing 5.00 mg Al^{3+} L^{-1} for 24 h. The solution was then removed by filtration (cellulose acetate filter - porosity 45 μm) and then continuously washed with a solution containing 1.50 mg Al^{3+} L^{-1} until the difference in the solution Al^{3+} concentration before and after filtration reached zero.

Scanning electron microscopy/energy dispersive X-ray spectroscopy (SEM/EDX) was performed with a model JSM-6390LV (JOEL USA Inc., Peabody, Massachusetts, USA), utilizing a "gold sputtering" technique at 10 kV. The infrared analyses were performed by Fourier Transform (FTIR), utilizing a model Spectrum 400 (PerkinElmer Inc., Waltham, Massachusetts, USA), and by the dispersive technique in potassium bromide (KBr) pellets, utilizing a model Prestige 21 (Shimadzu Corporation, Nakagyō-ku, Kyoto, Japan).

3. Results

3.1. Al^{3+} removal and pH studies

The first removal experiment was performed with 0.80 g L^{-1} of chitin, according to our previous work [15], and a number of synthetic solutions containing different Al^{3+} concentrations (Fig. 1). This amount completely removed the Al^{3+} in all tested concentrations, except for the most concentrated solution, containing 2.75 mg Al^{3+} L^{-1}, which had a 98% removal percentage. Thus, an experiment with lower chitin content (0.15 g chitin L^{-1}) was performed. This amount showed very satisfactory removal percentages (94% on average) for initial Al^{3+} concentrations equal to or lower than 2.00 mg L^{-1}, with all final solutions

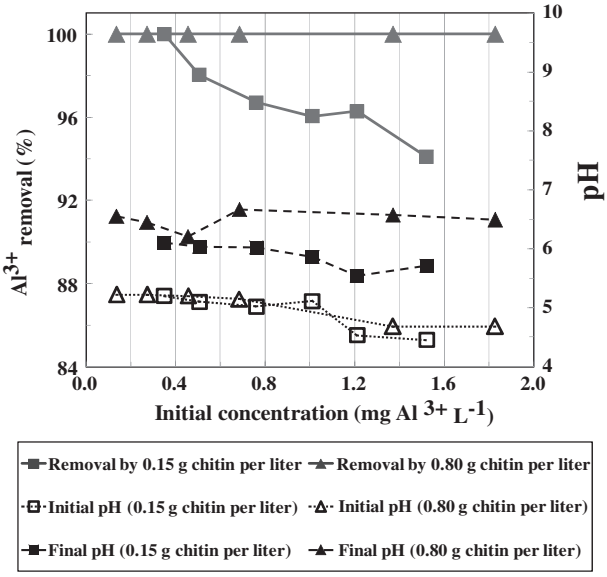

Fig. 1. Al^{3+} removal (%) and pH variation during synthetic solution removal experiments.

showing Al^{3+} concentrations below the WHO maximum allowed value, of 0.20 mg Al^{3+} L^{-1} [7].

An increase in the solution pH values was observed in the course of all removal experiments. Values varied from 4.9 to 5.9 in the assays with 0.15 g chitin L^{-1}, and from 4.9 to 6.3 in the assays with 0.80 g chitin L^{-1}, on average. The more concentrated the Al^{3+} initial and final solutions were, the lower the pH. This was credited to the Lewis acid characteristic of aluminum ions, which reduce solution pH. As the ion is removed from solution by chitin, the solution pH tends to increase, reaching a value of approximately 6.4 when the Al^{3+} removal from the solution is complete. This can be noted when comparing the rising pH values of both experiments (Fig. 1).

Based on the results with the synthetic solutions, Al^{3+} removal experiments with well water samples were carried out. The well water used in the experiments is from a drinking water source in a town located in southern Brazil and shows a high aluminum content (Table 1).

Due to the presence of cationic species other than aluminum in well water, such as iron and manganese, which could also be removed by chitin, the first removal assay was carried out with higher chitin content, 2.00 g L^{-1}. Al^{3+} removal was complete with this chitin content, and the same occurred when a quantity of 0.80 g chitin L^{-1} was tested, which was the optimal amount in the previous experiments in synthetic solutions. With these chitin amounts, the Fe_t removals were 98 and 94%, respectively, whereas the Mn_t removals were 68 and 58%.

Table 1
Measured concentrations of Al^{3+}, Fe_t, Mn_t, SiO_2, and SO_4^{2-} in well and DWTP water

Sample		
Species (mg L^{-1})	Well water	DWTP water
Al^{3+}	0.83	0.14
Fe_t	0.04	0.06
Mn_t	0.025	0.125
SiO_2	8.75	9.23
SO_4^{2-}	26.0	90.5

To evaluate potential competition between Al^{3+} and Fe/Mn species by the chitin sites, analogous experiments were carried out with other water samples with lower Al^{3+} and higher Fe/Mn contents than the well water. Therefore, a prefiltered DWTP sample, whose composition is also shown in Table 1, was selected. In this assay, because the DWTP water showed a lower Al^{3+} concentration (0.14 mg Al^{3+} L^{-1}), only 0.15 g chitin L^{-1} was used, to keep the chitin/Al^{3+} ratio consistent with respect to the well water experiment. This amount of chitin did not satisfactorily remove Al^{3+} from the solutions, with an average removal percentage of 25%. In contrast, 99% of the Fe_t was removed. This result shows a competition between aluminum and iron with respect to chitin, which can be explained by either a higher affinity of chitin for iron or by the presence of interfering substances in the water (e.g. humic substances). Consequently, the iron content of natural waters must be considered to determine the optimal amount of chitin for total aluminum removal.

The average Mn_t removal was lower than 70% in all cases, showing a lower affinity of chitin to this metal ion, which is most likely due to its larger size with respect to iron and aluminum. The average removal of silica was lower than 40% in all experiments. The concentration of sulfate was higher in DWTP than in well water because of the use of alum as a coagulant. However, the average sulfate removal by chitin in DWTP water was negligible and lower than 20% in well water, showing that chitin is not an adequate removal agent for this ion. Thereby, the removal experiments indicate that chitin is a promising agent for removing aluminum and iron ions from aqueous solutions. The results and standard deviations of the removal experiments are shown in Fig. 2.

3.2. Isothermal studies

Isothermal experiments were carried out in synthetic solutions with 0.15 g L^{-1} chitin, based on the

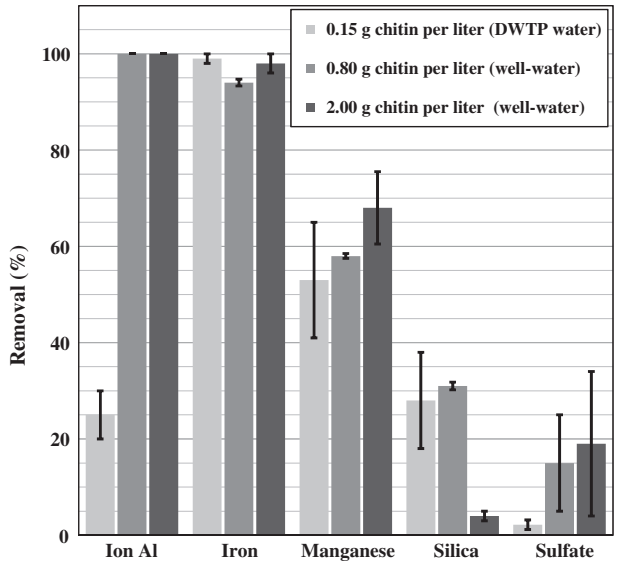

Fig. 2. Removal (with standard deviation) of Al^{3+}, Fe_t, Mn_t, SiO_2, and SO_4^{2-} in well and DWTP water.

Al^{3+} removal results, to obtain measurable residual Al^{3+} concentrations at equilibrium after the assays. In our previous paper [15], the Freundlich, Langmuir, and Sips models were applied to the experimental data, and a better agreement with the Sips model was determined, which is consistent with physisorption (Freundlich) and chemisorption (Langmuir) mechanisms at very low and at higher Al^{3+} concentrations, respectively. However, the R^2 and error values for the different models were close, and, consequently, we include one more model in this study (the Tóth model) and five error functions. The Tóth model is consistent with a chemisorption mechanism with weaker adsorbent/adsorbate interactions than the Langmuir model.

The model's equations and their respective linearizations are summarized in Table 2. The adsorption capacity for each concentration at equilibrium is given by q_e (in mg Al^{3+} g^{-1} of chitin), C_0 and C_t are the initial and at time t (in min) Al^{3+} concentrations (in mg Al^{3+} L^{-1}), respectively. K_L (L mg^{-1}), K_F (L g^{-1}), K_S (L mg^{-1}) and K_T (mg g^{-1}) are the constants of each model. The term $1/n$ is the Freundlich isotherm exponent, m the Sips isotherm exponent, α_T the Tóth isotherm constant, and $1/t$ the Tóth isotherm exponent. The isotherm model that best fits the experimental data was chosen by comparing the coefficient of correlation (R^2) for the models' linearized forms (higher values) and by comparing five different error functions between the experimental data and each model (lower values).The error functions analyzed were the sum of the square errors (ERRSQ), sum of absolute errors (EABS), average relative errors (ARE), hybrid fractional error function (HYBRID), and Marquardt's percent standard deviation (MPSD).The functions are shown in Table 3. The ERRSQ error function was used to apply the Microsoft Excel Solver add-in program to the Sips and Tóth models [16].

Fig. 3 shows the experimental data and the Langmuir, Freundlich, Sips, and Tóth curves for the data. It can be clearly observed that the Freundlich model does not fit the experimental data, while the Langmuir, Sips, and Tóth models are more likely to describe the data. This indicates that the removal is more prone to chemisorptive processes. The final parameters for all isothermal models, coefficients of correlation, and error values are listed in Table 4.

The coefficient of correlation had a slightly higher value for the Langmuir model ($R^2 = 0.9803$, compared to $R^2 = 0.9755$ for the other models). However, the error values for EABS, ERRSQ, and ARE showed lower values for the Tóth model (5.71256, 7.11845, and 16.14859, respectively), while HYBRID and MPSD were lower for the Freundlich model (47.51512 and 41.91367, respectively), which was previously discarded (Fig. 3). In addition, it has been shown that

Table 2
Isothermal model equations and respective linearizations

Isothermal models		
Model	Equation	Linearization
Langmuir	$q_e = \frac{q_{max} K_L C_e}{1 + K_L C_e}$	$\frac{C_e}{q_e} = \frac{1}{q_{max} K_L} + \frac{C_e}{q_{max}}$
Freundlich	$q_e = K_F C_e^{1/n}$	$\log q_e = \log K_F + \frac{1}{n} \log C_e$
Sips	$q_e = \frac{q_{max} K_S C_e^m}{1 + K_S C_e^m}$	$m \ln C_e = -\ln(K_S/q_e) + \ln(K_S)$
Tóth	$q_e = \frac{K_T C_e}{(a_T + C_e)^{1/t}}$	$(\ln(q_e/K_T) = \ln(C_e) - \frac{1}{t}\ln(a_T + C_e)$

Table 3
Error functions applied in the isothermal studies

Error functions	
ERRSQ	$\sum_{i=1}^{p} (q_{e,exp.} - q_{e,cal.})_i^2$
ARE	$\frac{100}{p} \sum_{i=1}^{p} \left(\frac{\lvert q_{e,exp.} - q_{e,cal.} \rvert}{q_{e,exp.}} \right)_i$
EABS	$\sum_{i=1}^{p} \lvert q_{e,exp.} - q_{e,cal.} \rvert_i$
HYBRID	$\frac{100}{p-n} \sum_{i=1}^{p} \left[\frac{(q_{e,exp.} - q_{e,cal.})^2}{q_{e,exp.}} \right]_i$
MPSD	$100 \left[\sqrt{\frac{1}{n-p} \sum_{i=1}^{p} \left(\frac{q_{e,exp.} - q_{e,cal.}}{q_{e,exp.}} \right)_i^2} \right]$

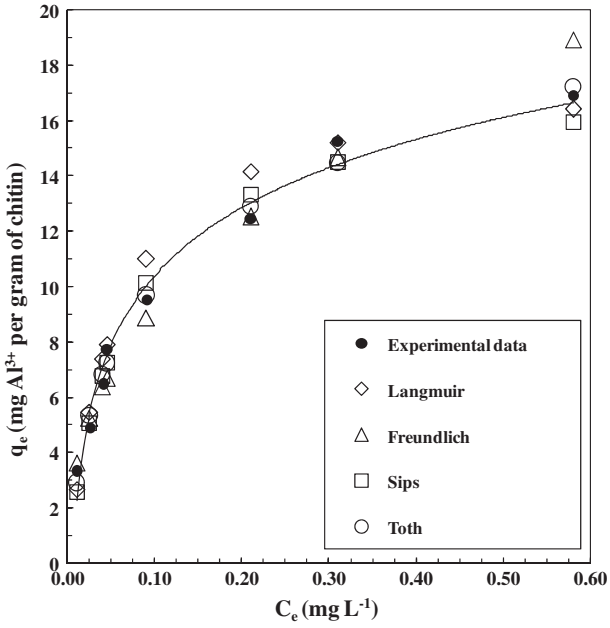

Fig. 3. Plot of experimental data and isothermal models for chitin.

the reliability of these errors decreases as their values increase [16,17].

It was therefore concluded that chitin is best represented by the Tóth model's premises. According to this model, the maximum removal capacity of the chitin is 20.14 mg Al^{3+} g^{-1}. The model assumes chemisorption processes between Al^{3+} and chitin, but chemical interactions of lower energy than those presented by the Langmuir model. Infrared spectroscopic analyses of chitin samples before and after the adsorption experiments given below are in agreement with this study. This adsorption is comparable to those found for chitosan, 21.3 mg g^{-1} [18], and for refused beach cast seaweed, of 22.5 mg g^{-1} [9]. On the other hand, chitin showed an adsorption capacity approximately two times higher than that found for rice husk char (9.78 mg Al^{3+} g^{-1}) [12]. The results confirm then that chitin is a very suitable Al^{3+} removal agent, with very promising applications for this purpose.

3.3. Kinetic studies

As chemisorption processes are credited as being the main removal process of Al^{3+} by chitin, it should be possible to rapidly remove Al^{3+} from solution. This fact was confirmed by kinetic experiments.

Kinetic experiments were carried out with 0.80 and 0.15 g chitin L^{-1} in synthetic solution (C_0 = 0.30 and 0.69 mg Al^{3+} L^{-1}, respectively) and with 0.80 and 2.00 g chitin L^{-1} in well water (C_0 = 0.83 mg Al^{3+} L^{-1}). Fig. 4 shows the Al^{3+} concentration variation (C_t/C_0) in all experiments plotted against the time of contact with the biopolymer. In synthetic solutions containing an initial concentration of 0.69 mg Al^{3+} L^{-1}, an amount of 0.15 g chitin L^{-1} was able to remove all aluminum ions in the solution in approximately 250 min in the analyzed conditions. With an initial concentration of 0.30 mg Al^{3+} $L^{-1}$and 0.80 g L^{-1} of chitin, complete Al^{3+} removal was reached in 10 min. In well water containing 0.83 mg Al^{3+} L^{-1}, complete Al^{3+} removal occurred in 40 and 150 min with 2.00 and 0.80 g chitin L^{-1}, respectively. The WHO allowed Al^{3+} level was reached in this water after 10 and 20 min with 2.00 and 0.80 g chitin L^{-1}, respectively. These results demonstrate that chitin is a highly efficient agent for the removal of Al^{3+}, efficiently removing relatively high amounts in short time periods.

Kinetic models were tested in this study to identify the predominant adsorption mechanism and evaluate its compatibility with the isothermal findings. Three different kinetic models have been used extensively in literature: pseudo-first-order, pseudo-second-order and intra-particle diffusion [19,20]; their equations and respective linearizations are shown in Table 5.

Data analysis for the pseudo-first-order model showed that the coefficient of correlation for the linearization resulted in values below 0.9723, while for the pseudo-second-order model, values equal to or higher than 0.9998 were obtained (Table 6), indicating that the pseudo-second-order model is more compatible with the experimental data in the synthetic solution and well water. The coefficient of correlation for the intraparticle diffusion model showed the lowest values, all below 0.5731, which demonstrates that

Table 4
Error results for isothermal models and respective parameters

Coefficient of correlation and error function results									
	R^2	EABS	ERRSQ	ARE	HYBRID	MPSD	Parameters		
Langmuir	0.9803	8.31190	12.29622	19.90408	52.08302	43.09792	q_{max} (mg g^{-1}) = 18.05	K_L (L mg^{-1}) = 17.31	–
Freundlich	0.9755	7.51211	11.71648	17.24182	47.51512	41.91367	n = 2.45	K_F (L g^{-1}) = 23.66	–
Sips	0.9755	7.23333	9.02040	17.84152	54.91230	46.31642	q_{max} (mg g^{-1}) = 18.25	K_S (L mg^{-1}) = 11.46	m = 0.922
Tóth	0.9755	5.71256	7.11845	16.14859	50.81097	45.50032	a_t = 0.02	K_T (mg g^{-1}) = 20.14	t = 1.319

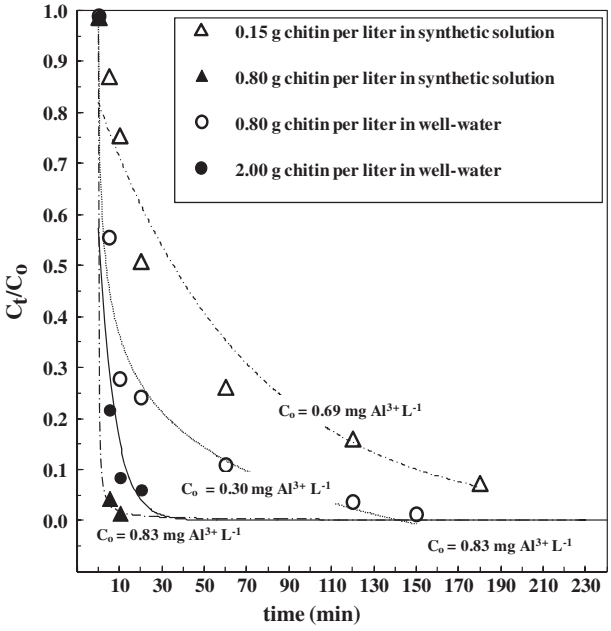

Fig. 4. Kinetic experiment results in synthetic solution and well water.

intraparticle diffusion does not take place in the adsorption process on the chitin biopolymer.

An excellent agreement between the pseudo-second-order model and the experimental data can be visualized in the graphical comparison shown in Fig. 5. The kinetic parameters and correlation coefficients for the pseudo-second-order models are shown in Table 6. One parameter of interest for comparison in the pseudo-second-order model is the initial rate of adsorption h. This initial rate was 0.1809 mg g^{-1} L^{-1} with 0.15 g chitin L^{-1} in synthetic solution (C_0 = 0.69 mg Al^{3+} L^{-1}), and it was 37 times higher when 0.80 g chitin L^{-1} was employed with an initial concentration of 0.30 mg Al^{3+} L^{-1}. In well water, a small increase in the initial rate was observed with an increase in chitin content, and an h value of 0.6328 mg g^{-1} L^{-1} was obtained for 2.00 g chitin L^{-1}. This fact can be explained by the presence in well water of substances that interfere with the Al^{3+} adsorption process, as discussed above.

The pseudo-second-order kinetic model indicates that the adsorption of Al^{3+} by the biopolymers is dependent on the ion's concentration in the adsorbent and on the equilibrium concentration of the adsorbate. This model is consistent with a controlling kinetic mechanism via chemical adsorption, confirming the previous isothermal study results.

3.4. Continuous regime studies

Experiments in descending flow columns were performed with well water, aiming to find the best contact time between chitin and the water, the optimal flow rate for removal and the saturation of the adsorbent. The parameters applied for all column experiments can be observed in Table 7.

Table 5
Kinetic equations and respective linearizations

Kinetic models		
Model	Equation	Linearization
Pseudo first-order	$q_t = q_e - \frac{q_e}{10^{K_1 t/2.303}}$	$\log(q_e - q_t) = \log q_e - K_1 t$
Pseudo second-order	$q_t = q_e \frac{q_e K_2 t}{1+q_e K_2 t}$	$\frac{t}{q_t} = \frac{1}{K_2 q_e^2} + \frac{t}{q_e}$
Intra-particle diffusion	$q_t = K_D t^{1/2}$	–

Table 6
Kinetic parameters and correlation coefficients for the pseudo-second-order model

	0.80 g chitin L^{-1} C_0 = 0.30 mg Al^{3+} L^{-1} synthetic solution	0.15 g chitin L^{-1} C_0 = 0.69 mg Al^{3+} L^{-1} synthetic solution	0.80 g chitin L^{-1} C_0 = 0.83 mg Al^{3+} L^{-1} well water	2.00 g chitin L^{-1} C_0 = 0.83 mg Al^{3+} L^{-1} well water
Final kinetic parameters	$t/q_t = 1.1631t + 0.1404$	$t/q_t = 0.2126t + 5.5264$	$t/q_t = 0.9602t + 5.0828$	$t/q_t = 0.4083t + 1.5804$
R^2	0.9999	0.9998	~1	~1
K_2 (g mg^{-1} min^{-1})	9.6353	0.0082	0.1814	3.6699
h (mg g^{-1} min^{-1})	7.1225	0.1809	0.1967	0.6328
$q_{e,\ exp}$ (mg g^{-1})	0.8625	4.6000	1.0375	0.4150
$q_{e,\ calc}$ (mg g^{-1})	0.8698	4.7000	1.0414	0.4152
ERRSQ	0.14254	0.14514	0.00938	0.00452

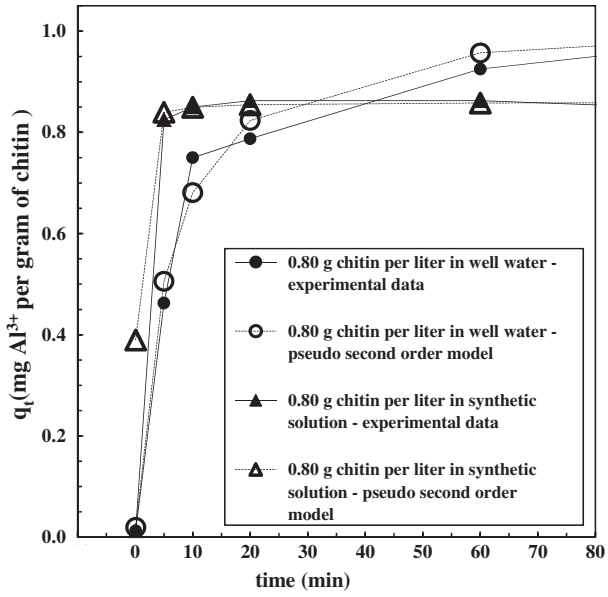

Fig. 5. Comparison between experimental data and pseudo-second-order kinetic models.

It was established, from the kinetic experiments, that the minimum chitin/well water contact time for reaching the WHO-allowed Al^{3+} level is approximately 20 min. For this purpose, the column was first filled with 5.00 g of chitin, and a flow rate of 2.50 mL min^{-1} was applied, resulting in a contact time of approximately 28 min. At these conditions, complete Al^{3+} removal was achieved after 24 h of completion of the experiment. Due to high aluminum removal in the previous experiment, the following assay was conducted with a sharply decreased amount of chitin (1.40 g), and the flow rate was increased (to 14.2 mL min^{-1}), resulting in a contact time of 1.40 min. This experiment completely removed Al^{3+} after 2 h, and kept it below the maximum WHO-allowed value for at least 12 h of the experiment.

One last experiment, aiming to saturate chitin with aluminum, was prepared with 0.55 g of chitin and a flux approximately 30% higher (19.8 mL min^{-1}) than in the previous experiment. These parameters allowed a contact time of 0.40 min (24 s) and a hydraulic application rate of 6.71 m^3 m^{-2} h^{-1}. These conditions maintained the effluent Al^{3+} concentration below the WHO-allowed level for 35 min, and chitin saturation ($C_t = C_0$) was reached in 780 min.

Table 7
Parameters in the column experiments

Experiments	1	2	3
Chitin amount (g)	5.00	1.40	0.55
Flux (mL min^{-1})	2.50	14.20	19.80
Hydraulic application rate (m^3 m^{-2} h^{-1})	0.84	2.75	6.71
Reactor volume (cm^3)	70	19.8	7.8
Experiment time (min)	1,440	720	780
Hydraulic retention time (min)	28	1.4	0.4

The maximum quantity of Al^{3+} that could be absorbed by the chitin in a continuous descending flow column was calculated from the last experiment's data in which the saturation of chitin was attained. The adsorption capacity of Al^{3+} by chitin q (mg g^{-1}) in the experiment can be calculated according to Eq. 1 [21], where Q is the flow (mL min^{-1}), C_o the affluent Al^{3+} concentration (mg L^{-1}), and w the dry chitin mass (g). The function $f(t)$ is the curve obtained from plotting the experimental data C_t/C_0 over time (Fig. 6). Its equation, $f(t) = 10^{-9}t^3 - 2.10^{-6}t^2 + 0.001t + 0.11$, was obtained from the Microsoft Excel computer program. The term t_b is the time to breakthrough and t_e is the time to exhaustion (both in min). The t_b and t_e times from the experiment were 1 and 780 min, respectively (Fig. 6). The adsorbed Al^{3+} quantity in the experiment is represented by the shaded area of Fig. 6, corresponding to the term $(t_e - \int_{t_b}^{t_e} f(t)dt)$ in Eq. 1. The result of this equation is the maximum adsorption capacity, 9.53 mg Al^{3+} g^{-1} of chitin.

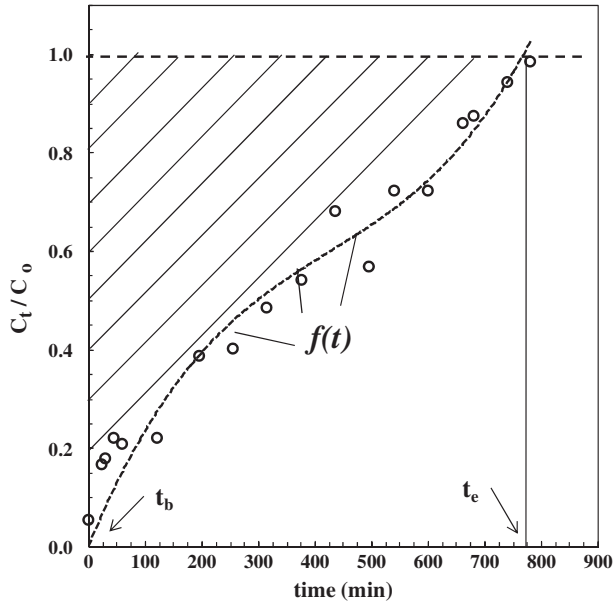

Fig. 6. Plot of the Al^{3+} experimental data C_t/C_0 over time for the experiment 3 (0.55 g of chitin; well water: 0.83 mg Al^{3+} L^{-1}, flux 19.80 mL min^{-1}).

$$q = \frac{(t_e - \int_{t_b}^{t_e} f(t)dt)QC_0}{w} \quad (1)$$

The Fe_t, Mn_t, silica, and sulfate concentrations from last experiment were also evaluated. The Fe_t concentration in the well water was initially 0.009 mg L^{-1}, which was then reduced to 0.004 mg L^{-1} after 780 min (~56% removal). The Mn_t concentration was reduced from 0.013 to 0.011 mg L^{-1} (~15% removal). The concentrations of sulfate (25 mg L^{-1}) and silica (~10 mg L^{-1}) did not significantly decrease during the test period.

The column experiments showed that chitin has a high and fast Al^{3+} removal ability in continuous experiment conditions. The calculated chitin removal capacity in the column experiment was less than that calculated in the study of isotherms in the batch system ($q_{max} = 20.14$ mg g^{-1}, Table 4) because well water contains other substances that compete or interfere with chitin's adsorption sites, such as iron, manganese, humic substances, etc. A comparison of chitin's removal capacity under continuous flux experiments with other sorbents related to the Al^{3+} removal ability is difficult, due to the different experimental conditions applied in other works. However, column studies with seaweed algae as an adsorbent [9] and wastewater containing aluminum showed maximum adsorption values of 12 mg Al^{3+} per gram of adsorbent in column studies.

3.5. SEM/EDX analysis

SEM/EDX analysis was performed to study the surface of chitin and identify the elements present in the surface of the analyzed samples before and after saturation with Al^{3+} from a concentrated synthetic solution. The following figures show the results, with magnifications varying from 50 to 4,000 times.

It can be observed that the chitin surface is quite smooth, as observed in Fig. 7(a) (magnification 50×). However, in Fig. 7(b) (magnification 4,000×), crystalline incrustations were observed, and EDX analysis demonstrated high concentrations of calcium and phosphorus on the surface of the sample. This demonstrates that the chitin used in the experiments is not pure, and still contains phosphate and calcium residues from the shrimp shells. However, after contact of the chitin with the solution containing Al^{3+}, a sharp decrease in the number of incrustations was observed, which is most likely due to a dissolution process promoted by the slightly acidic Al^{3+} solution.

The chitin surface after saturation with Al^{3+} is shown in Fig. 8. The formation of needle-shaped crystal structures on the surface can be observed in Fig. 8(a) (magnification 500×); these were not previously observed in the prepared chitin before contact with Al^{3+} solution. EDX analysis revealed the presence of sulfur in this area, due to the use of alum in the preparation of the synthetic solution. At a greater magnification of 4,000×, crystalline structures forming distinct shapes can be observed, as shown in Fig. 8(b). The EDX analysis of these incrustations revealed a peak of aluminum, demonstrating that this element is present in considerable quantities on those structures, suggesting the presence of adsorption sites along the surface [18].

3.6. Infrared analysis

Infrared spectra were collected for chitin and Al^{3+}-saturated chitin from synthetic solution and well water. FTIR and dispersive techniques showed the same results, and the spectra are shown in Fig. 9. Infrared spectroscopy enables the visualization of the presence of covalent bonds between substances in the sample. Modifications in the chitin spectrum bands after saturation with aluminum or the appearance of new bands would demonstrate whether the formation of strong chemical bonds occurred between aluminum and chitin, facilitating the identification of coordination compounds.

In the free chitin spectrum, bands can be observed in the region 3,600–2,800 cm^{-1}, which is characteristic

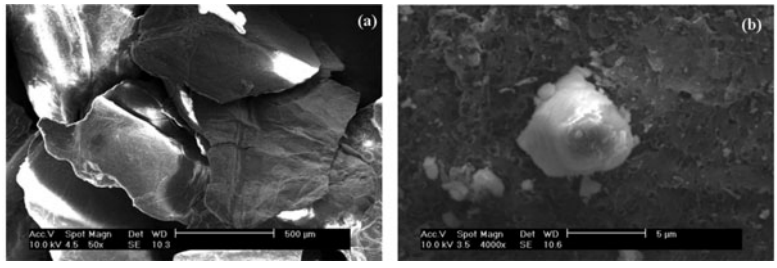

Fig. 7. SEM micrographs of: (a) chitin surface (50x); and (b) calcium and phosphorus structures on chitin surface (4000x).

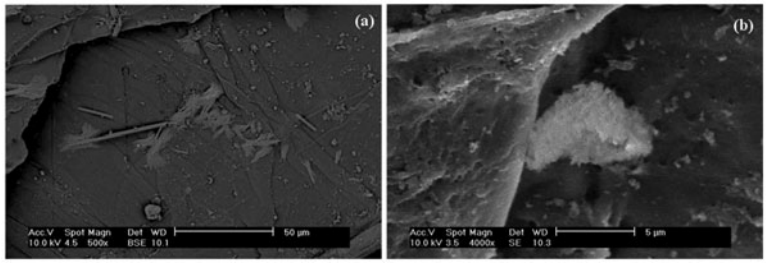

Fig. 8. SEM micrographs of chitin saturated with Al^{3+}: (a) crystal needles on chitin surface (500x); (b) crystal structures containing high Al^{3+} concentration on chitin surface (4000x).

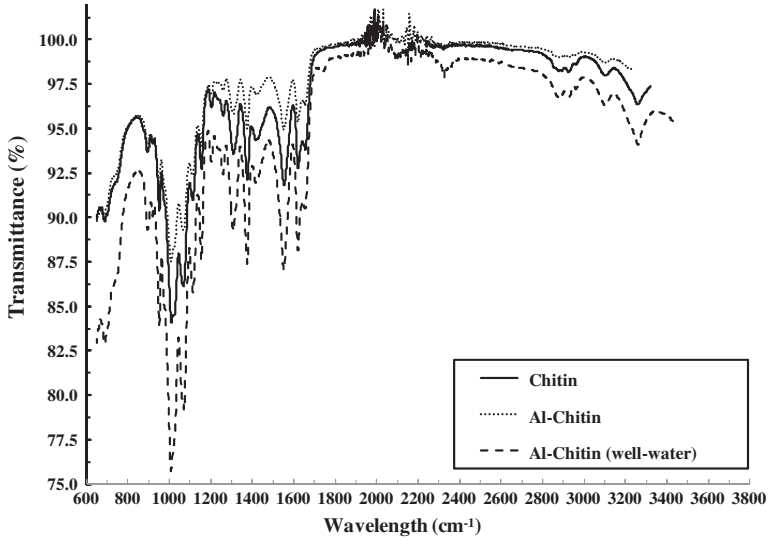

Fig. 9. Infrared spectra of the prepared chitin and Al^{3+}-saturated chitin with synthetic solution and well water.

of υ(O–H), υ(N–H), and υ(C–H) stretching; these bands are broad and somewhat reduced compared to other chitin spectra [22]. This fact is indicative of the presence of impurities in the chitin used, as observed in the previous SEM/EDX analysis. Stretching vibrations υ(OH) of the hydroxyl groups appear in a wide band centered at 3,480 cm^{-1}, indicating several types of hydroxyl groups in the molecule.

The spectrum shows the characteristic bands of the secondary amide group; tension and deformation bands of the group N–H at υ(NH) = 3,259 cm^{-1} and δ(NH) = 1,621 cm^{-1}, respectively; stretching bands of the carbonyl group at υ_a(CO) = 1,656 and υ_s(CO) = 1,556 cm^{-1}; and the stretching vibration υ(CN) at 1,203 cm^{-1} are also evident; the band at 1,379 cm^{-1} is assigned to the deformation δ_a(CH) of the methyl group of the acetamide group. The band at 1,070 cm^{-1} is related to the stretching of the C–O–C bond, corresponding to the bonds between monomers in the polymer. The position of the bands υ_a(CO) and δ(NH) suggests that the chitin used corresponds to the polymorphous form β [22].

The spectra of samples containing aluminum were consistent with the free chitin spectrum, showing no significant changes in intensity or position in any band. It can therefore be concluded that there are no strong chemical bonds between chitin and aluminum, and the possibility of the formation of coordination compounds between Al^{3+} and the functional groups of chitin can be discarded. This result is in agreement with the isothermal studies, from which the chemisorption mechanism via the Tóth model, with chemical interactions weaker than those corresponding to covalent bonds was proposed.

4. Conclusions

Chitin was capable of removing Al^{3+} from synthetic solutions and well water, in both batch and continuous regimes, in short times and with a high adsorption capacity.

The isothermal studies revealed that Al^{3+} removal by chitin best fits the Tóth model, which is consistent with a chemisorption mechanism with weak interactions between the sorbent and sorbate. A maximum removal capacity of 20.14 mg Al^{3+} g^{-1} of chitin was calculated, a value comparable to or higher than values reported for other adsorbents. The presence of chemical interactions between Al^{3+} and chitin was confirmed by the kinetic studies, from which a pseudo-second-order model with a high initial adsorption rate was deduced.

SEM/EDX analysis revealed impurities on the utilized chitin and adsorption sites along the surface after contact with aluminum. Infrared spectroscopy demonstrated that there are no covalent bonds between aluminum and chitin, negating the formation of Al–chitin coordination compounds and confirming the isothermal findings.

The competition of some species present in natural waters, such as iron and manganese, with aluminum in the adsorption sites of chitin was demonstrated. Descendent flow column experiments yielded a calculated removal capacity of 9.53 mg Al^{3+} per g of chitin in the analyzed well water (0.83 mg Al^{3+} L^{-1}), a lower amount than in batch experiments with synthetic solution, confirming that species interfering with aluminum must be considered to attain total aluminum removal from natural waters. This removal capacity means that 1 kg of chitin could treat approximately 12 m^3 of this well water, a sufficient amount to supply aluminum-free water for drinking and cooking to a family of four members for approximately 10 months with a low cost. Thus, this research can contribute to a solution for the serious problem of direct well water consumption containing high levels of aluminum, which is very common in southern Brazil.

From the above results, it can be concluded that chitin is a very suitable agent for Al^{3+} removal from synthetic solutions and well water. Hence, large-scale applications, as well as chitin regeneration experiments, will be carried out in the next stage of this research.

Acknowledgments

The authors would like to acknowledge CAPES and FAPESC for their support and sponsorship, and SAMAE (Araranguá, Santa Catarina, Brazil) for providing well water samples to complete this work.

Symbols

C_0	—	initial concentration (mg L^{-1})
C_e	—	concentration at equilibrium (mg L^{-1})
C_t	—	concentration at time t (mg L^{-1})
q_e	—	adsorption capacity at equilibrium (mg g^{-1})
q_t	—	amount adsorbed at time t (mg g^{-1})
K_L	—	Langmuir constant (L mg^{-1})
K_F	—	Freundlich constant (L g^{-1})
K_S	—	Sips constant (L mg^{-1})
K_T	—	Tóth constant (mg g^{-1})
K_1	—	pseudo-first-order model constant (min^{-1})
K_2	—	pseudo-second-order model constant (g mg^{-1} min^{-1})
K_d	—	intra-particle constant (g mg $min^{-1/2}$)
h	—	initial adsorption rate (mg g^{-1} min^{-1})
$1/n$	—	Freundlich isotherm exponent
m	—	Sips isotherm exponent
α_T	—	Tóth isotherm constant
$1/t$	—	Tóth isotherm exponent
Q	—	flow (mL min^{-1})
w	—	dry chitin mass (g)
t_b	—	time to breakthrough (min)
t_e	—	time to exhaustion (min)
WHO	—	World Health Organization
DWTP	—	drinking water treatment plant
FTIR	—	Fourier transform infrared
SEM/EDX	—	scanning electron microscopy/energy dispersive X-ray spectroscopy
ERRSQ	—	sum of the square errors
EABS	—	sum of absolute errors
ARE	—	average relative errors
HYBRID	—	hybrid fractional error function
MPSD	—	Marquardt's percent standard deviation

References

[1] ATSDR-Agency for Toxic Substances and Disease Registry, Aluminum—Potential for Human Exposure, Department of Health and Human Services (2009), U.S. 175–227.
[2] M.S. Kim, L.S. Clesceri, Aluminum exposure: A study of an effect on cellular growth rate, Sci. Total Environ. 278 (2001) 127–135.
[3] S.C. Bondy, The neurotoxicity of environmental aluminum is still an issue, Neurotoxicol. 31 (2010) 575–581.
[4] W.F. Forbes, J.F. Gentleman, Risk factors, causality, and policy initiatives: The case of aluminum and mental impairment, Exp. Gerontol. 33 (1998) 141–154.
[5] J.R. Walton, Aluminium in hippocampal neurons from humans with Alzheimer´s disease, Neurotoxicol. 27 (2006) 385–394.
[6] G. Berthon, Aluminium speciation in relation to aluminum bioavailability, metabolism and toxicity, Coord. Chem. Rev. 228 (2002) 319–341.

[7] WHO-World Health Organization, Aluminum in Drinking Water, in: Guidelines for Drinking-water Quality, Geneva, 2003.
[8] A. Denizli, R. Say, E. Piskin, Removal of aluminum by Alizarin Yellow-attached magnetic poly(2-hydroxyethyl methacrylate) beads, React. Funct. Polym. 55 (2002) 99–107.
[9] P. Lodeiro, A. Gudiña, L. Herrero, R. Herrero, M.E.S. De Vicente, Aluminum removal from wastewater by refused beach cast seaweed, J. Hazard. Mat. 178 (2010) 861–866.
[10] M.N. Othman, P. Abdullah, Y.F.A. Aziz, Removal of aluminum from drinking water, Sains Malaysiana 39 (2010) 51–55.
[11] E. Rodil, R. Dumortier, J.H. Vera, Removal of aluminum from aqueous solutions using sodium di-(n-octyl) phosphinate, Chem. Eng. J. 97 (2004) 225–232.
[12] T.S. Singh, B. Parikh, K.K. Pant, Investigation on the sorption of aluminum in drinking water by low cost adsorbents, Water SA 32 (2006) 49–54.
[13] V.V.C. Azevedo, S.A. Chaves, D.C. Bezerra, M.V. Lia Fook, A.C.F.M. Costa, Chitin and chitosan: Application as biomaterials, Electron. Mag. Mater. Process. 23 (2007) 27–34.
[14] M.A. Lobo-Recio, A.L.R. Mercê, M.E. Nagel-Hassemer, F.R. Lapolli, Aluminum in Waters Sources, Speciation and Removal Techniques, in: Molecular and Supramolecular Bioinorganic Chemistry: Applications in Medical and Environmental Sciences. Nova Science Publisher Inc., New York, NY, 2011.
[15] M.A. Lobo-Recio, F.R. Lapolli, T.J. Belli, C.T. Folzke, R.R.Z. Tarpani, Study of the removal of residual aluminum though the biopolymers carboxymethylcellulose, chitin and chitosan, Desalin. Water Treat. 51 (2013) 1735–1743.
[16] K.Y. Foo, B.H. Hameed, Insights into the modeling of adsorption isotherm systems, Chem. Eng. J. 156 (2010) 2–10.
[17] J.C.Y. Ng, W.H. Cheung, G. McKay, Equilibrium studies for the sorption of lead from effluents using chitosan, Chemosphere 52 (2003) 1021–1030.
[18] J.I. Simionato, A.T. Paulino, J.C. Garcia, J. Nozaki, Adsorption of aluminum from wastewater by chitin and chitosan produces from silkworm chrysalides, Polym. Int. 55 (2006) 1243–1248.
[19] C. Cojocaru, M. Diaconu, I. Cretescu, J. Savic, V. Vasic, Biosorption of copper(II) ions from aqua solution using dried yeast biomass, Colloids Surf. A. 335 (2009) 181–188.
[20] A. Witek-Krowiak, R.G. Szafran, S. Modelski, Biosorption of heavy metals from aqueous solution onto peanut shell as a low-cost biosorbent, Desalination 265 (2011) 126–134.
[21] D. Zhou, L. Zhang, J. Zhou, S. Guo, Development of a fixed-bed column with cellulose/chitin beads to removal heavy-metals ions, J. Appl. Polym. Sci. 94 (2004) 684–691.
[22] M. Rinaudo, Chitin and chitosan: Properties and applications, Prog. Polym. 31 (2006) 603–632.